Available online at www.sciencedirect.com
SCIENCE DIRECT
Journal of Magnetic Resonance 178 (2006) 329–333
JMR Journal of Magnetic Resonance
www.elsevier.com/locate/jmr

Communication

The aqueous reference for ESR oximetry

Galina Diakova, Robert G. Bryant *

Chemistry Department, University of Virginia, Charlottesville, VA 22901, USA

Received 19 August 2005; revised 3 October 2005
Available online 26 October 2005

Abstract

The interaction of molecular oxygen with derivatives of nitroxide EPR spin labels has been investigated using nuclear spin-relaxation spectroscopy in aqueous and nonaqueous solvents. The proton spin–lattice relaxation rate induced by oxygen provides a measure of the local concentration of oxygen, which we find is dependent on solvent. In water, the hydrophobic effect increases the local concentration of oxygen in the nonpolar portions of solute molecules. For nitroxides reduced to the hydroxylamine in aqueous solutions, we find that the local concentration of oxygen is approximately twice that associated with a free diffusion hard sphere limit, while in octane, this effect is absent. These results show that nitroxide based ESR oximetry may suffer a reference concentration shift of order a factor of two if the aqueous nitroxide spectrum or relaxation is used as the reference.

Keywords: Oximetry; ESR; Spin relaxation; Nitroxides; Oxygen

1. Introduction

The use of nitroxide ESR to measure oxygen concentration has provided considerable information about the distribution of oxygen in a variety of heterogeneous biological environments [1–20]. The method depends on the change in the electron spin relaxation induced in nitroxide radicals by collisional encounters with oxygen. The relaxation rate is a linear function of the oxygen concentration, which is the basis for defining local oxygen concentrations.

A primary application is to biological systems that provide a complex mixture of different local environments such as the low dielectric environment of a membrane interior or the high dielectric aqueous cytosol. The oxygen collision probability may be affected by the local solute properties, and we investigate here the extent of the differences that may be expected for reduced nitroxides in aqueous compared with nonaqueous environments. The approach that we use is to explore the paramagnetic contributions to the proton spin–lattice relaxation rates of reduced nitroxides in water and in nonaqueous solvents and compare the differences with simple hard-sphere diffusional relaxation models in both cases. These nuclear spin-relaxation measurements show that the reduced nitroxide associates with oxygen more in water than in nonaqueous solutions. This observation implies that in structurally similar nitroxide molecules, the comparison of oxygen induced electron spin-relaxation rate changes between aqueous and nonaqueous environments require attention to this difference.

2. Experimental

TEMPO derivatives 4-hydroxy-2,2,6,6 tetramethylpiperidine-1-oxyl (4-hydroxy-TEMPO), 4-carboxy-2,2,6,6 tetramethylpiperidine-1-oxyl (4-carboxy-TEMPO), 4-amino-2,2,6,6 tetramethylpiperidine-1-oxyl (4-amino-TEMPO), sodium hydrosulfite, and phenylhydrazine were purchased from Sigma–Aldrich Chemical (St. Louis, MO, USA), deuterated solvents were obtained from Cambridge Isotope Laboratories (Andover, MA, USA). Compressed gases were purchased from Messer MG Industries (Malvern, PA, USA).

The hydroxylamine derivatives of the hydroxyl-, carboxyl-, and amino-nitroxides were prepared by reduction with sodium hydrosulfite in situ [21]. For aqueous solutions, the

* Corresponding author. Fax: +1 434 924 3567.
E-mail address: rgb4g@virginia.edu (R.G. Bryant).

1090-7807/$ - see front matter © 2005 Elsevier Inc. All rights reserved.
doi:10.1016/j.jmr.2005.10.004

nitroxide was reacted with an equivalent amount of sodium hydrosulfite and NMR measurements were made several hours later at a nominal concentration of 50 mM of the hydroxylamine. Reduction of 4-hydroxy-TEMPO in chloroform was accomplished using phenylhydrazine as the reducing agent [22]. The hydroxylamine was recrystallized from chloroform and used for experiments in nonaqueous solvents at concentrations of approximately 15 mM in chloroform and 7 mM in octane.

Samples for NMR measurements were contained in Wilmad 524PP glass tubes (Buena, NJ, USA). Solutions were prepared using up to 6 freeze–pump–thaw cycles on a gas manifold and then loaded with oxygen or nitrogen at pressures determined by the gauge reading on a 2-stage regulator. Gas pressures were 11 atm in aqueous solutions, 3 atm in octane solutions, and air was used as the oxygen source for chloroform solutions because of the high oxygen solubility. NMR measurements were made using a Varian Unity Plus NMR spectrometer operating at 500 MHz and 25 °C. T_1 measurements were made using a standard inversion recovery sequence.

3. Results and discussion

The relaxation rate of the solute protons is enhanced by the presence of molecular oxygen; however, the local concentration of oxygen in water around a solute may vary as a function of the solute structure [23]. The paramagnetic contribution to the solute proton relaxation rate constant by a freely diffusing paramagnetic relaxation agent through a dipole–dipole coupling has been discussed in detail recently [23,24]. We note that while the electron–nuclear dipolar coupling may dominate the nuclear spin–lattice relaxation rate constant, the electron relaxation induced by oxygen in nitroxides is dominated by spin exchange mechanisms. The proton spin–lattice relaxation rate constant is linear in the paramagnet concentration and depends on a structural or steric factor that affects the uniformity of contact between the observed proton and the diffusing paramagnetic cosolute. In the present experiments, the cosolute is oxygen, which is small and sensitive to the local steric factors of the solute studied. To account for these steric factors, we compute a relaxation rate or the strength of the oxygen–proton dipolar coupling from a lattice model. Essentially we numerically integrate the dipolar coupling by summing $1/r^6$ contributions using a lattice of points about the solute molecules and presume that the oxygen concentration is uniform everywhere in the solution. The result is compared with a spherical hydrogen atom to provide a steric factor f between 0 and 1 that accounts for the molecular shape in modifying the effective distances of approach between the relaxation agent and the particular proton detected. In the present experiments, we normalize the relaxation rates for the solute protons to those detected for the solvent protons to provide a reference. At a particular magnetic field we may then write the relaxation equation

$$\frac{1}{T_{1k}} = BP\frac{[\mathrm{S}]}{bD}J, \tag{1}$$

where B defines the strength of the dipolar coupling, b, the distance of closest approach between the electron and nuclear spin, [S] the concentration of the electron spin, D the relative translational diffusion constant, and J the sum of spectral density functions evaluated at the resonance magnetic field strength which is a function of the electron relaxation time constant and the relative translational correlation time. Oxygen has an electron spin-relaxation time of ≈7.5 ps [25]. Because this correlation time is short, the correlation time for the electron–nuclear coupling is dominated by the electron spin-relaxation time and is only weakly a function of the relative translational correlation time. The relaxation rate constant is a function of the oxygen concentration and the factors that define the accessibility to the observed nuclear spins. For the kth proton site

$$P_k = f_k K_k, \quad K_k = [O_{2,\mathrm{local}}]/[O_{2,\mathrm{bulk}}], \tag{2}$$

where f_k is a geometric factor that accounts for the local bonding pattern in the molecule that limits uniform access to the detected nuclear spin compared with a spherically symmetric hydrogen atom. The ratio of concentrations in K_k is related to the free energy difference between the local environment of the solute proton and the bulk environment of the solvent proton. The paramagnetic contribution to the solvent protons provides a reference for Eq. (2). Then, the ratio of the paramagnetic contributions to the relaxation rate constants yields the concentration ratio, K, and the lattice sum calculations provide the steric factors, f.

$$\frac{R^{\mathrm{para}}_{1,\mathrm{solute}}}{R^{\mathrm{para}}_{1,\mathrm{solvent}}} = \frac{P_{\mathrm{solute}}BJ[O_{2,\mathrm{local}}]}{P_{\mathrm{solvent}}BJ[O_{2,\mathrm{bulk}}]} = \frac{f_{\mathrm{solute}}}{f_{\mathrm{solvent}}}K. \tag{3}$$

We summarize the steric factors for the solvent and solute protons in Table 1. In all cases the factors listed represent the average taken over all protons of that type, e.g., three for methyl groups. The values of K deduced from the ratio of the relaxation rate constants are summarized in Table 2 for aqueous solutions of the hydroxylamines obtained by reduction of the corresponding nitroxides. The values of K vary for different protons, but are close to 2 for most cases. The 4-carboxy values are larger, and the 4-amino values slightly smaller; however, the values of K are significantly different from unity.

Measurements in nonaqueous solvents are somewhat difficult for these compounds because of limited solubility and, in chloroform, time dependent oxidation of the hydroxylamine by oxygen to the corresponding nitroxide that is paramagnetic and which increases the solute and solvent proton relaxation rates. To overcome the effects of the oxidation, we measured the proton relaxation rates as a function of time, and extrapolated to zero to obtain an initial proton relaxation rate in the presence of oxygen, but not nitroxide. Data for chloroform solutions are shown

Table 1
Geometric factors

Compound	Proton	f
Hydrogen atom	Single proton	1.00
Water	Proton	0.59
Chloroform	Proton	0.36
n-Octane	CH_2	0.34
n-Octane	CH_3	0.45
4-Hydroxy-2,2′,6,6′-tetramethylpiperidine-*N*-hydroxylamine (**I**)	CH-R	0.26
	$CH_{2\,eq}$	0.30
	$CH_{2\,ax}$	0.26
	$CH_{3\,eq}$	0.35
	$CH_{3\,ax}$	0.33
4-Amino-2,2′,6,6′-tetramethylpiperidine-*N*-hydroxylamine (**II**)	CH-R	0.23
	$CH_{2\,eq}$	0.28
	$CH_{2\,ax}$	0.26
	$CH_{3\,eq}$	0.35
	$CH_{3\,ax}$	0.33
4-Carboxy-2,2′,6,6′-tetramethylpiperidine-*N*-hydroxylamine (**III**)	CH-R	0.22
	$CH_{2\,eq}$	0.28
	$CH_{2\,ax}$	0.22
	$CH_{3\,eq}$	0.35
	$CH_{3\,ax}$	0.33

Geometric factors for protons in tetramethylpiperidine-hydroxylamine and solvents calculated based on a 0.025 Å lattice; R is hydroxy-, amino-, or carboxy-group in the corresponding hydroxylamines.

Table 2
Relaxation summary

Compound	Proton	Shift (ppm)	$1/T_{1p}$ (s^{-1})	K
I	HOD	4.74s	1.63	
	C–H	4.25m	1.57	2.2
	$CH_{2\,eq}$	2.15m	1.67	2.0
	$CH_{2\,ax}$	1.55m	1.31	1.8
	$CH_{3\,eq}$	1.50s	1.73	1.8
	$CH_{3\,ax}$	1.47s	1.73	1.9
II	HOD	4.74s	1.67	
	C–H	3.90m	1.10	1.7
	$CH_{2\,eq}$	2.27m	1.25	1.6
	$CH_{2\,ax}$	1.80m	1.09	1.5
	$CH_{3\,eq}$	1.55s	1.66	1.7
	$CH_{3\,ax}$	1.52s	1.74	1.9
III	HOD	4.74s	1.85	
	C–H	2.86m	1.91	2.8
	$CH_{2\,eq}$	2.05m	2.08	2.4
	$CH_{2\,ax}$	1.63m	1.81	2.6
	$CH_{3\,eq}$	1.50s	1.91	1.8
	$CH_{3\,ax}$	1.46s	1.99	2.0

Summary of relaxation rates for protons at different chemical shifts in aqueous solutions of tetramethylpiperidine-hydroxylamine.

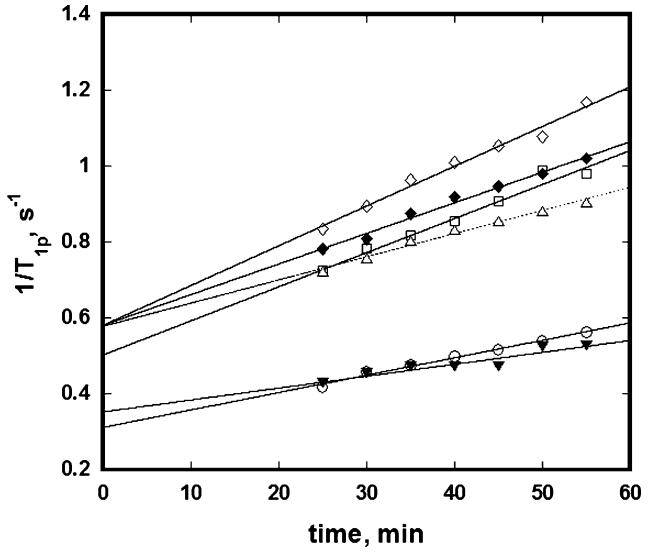

Fig. 1. The proton spin–lattice relaxation rate constants as a function of time for the protons in 4-hydroxy-2,2,6,6-tetramethylpiperidine-*N*-hydroxylamine in chloroform at a resonance frequency of 500 MHz: open circle, chloroform proton; open square, C-4 proton; open diamond, axial CH_2; filled diamond, equatorial CH_2; open triangle, CH_3 equatorial; and filled triangle, axial CH_3.

in Fig. 1 and the summary of relaxation results is presented in Table 3. The values of K in chloroform are similar to those in water; however, the values in *n*-octane, which may model a membrane interior, are the order of 1. Thus, in *n*-octane, the solvent and the solute experience the same local oxygen concentration, while in water and the chloroform, the solutes experience a higher local oxygen concentration than the solvent protons. The differences are of order a factor of 2.

The NMR measurements reported here are for the diamagnetic hydroxyl amine, which we take as a model for the corresponding nitroxide. An increase in the oxygen collision frequency or effective concentration in hydrophobic regions of solutes in water appears to be fairly general as measured by this proton spin-relaxation method [23,24]. In extrapolating the hydroxyl amine result to the nitroxide, the assumption is that the added proton and the associated

Table 3
Relaxation summary

Solvent	Proton	Shift (ppm)	$1/T_{1p}$ (s^{-1})	K
Chloroform	$CHCl_3$	7.24s	0.31	
	C–H	4m	0.50	2.2
	$CH_{2\,eq}$	1.92m	0.58	2.2
	$CH_{2\,ax}$	1.54m	0.58	2.5
	$CH_{3\,eq}$	1.2s	0.58	1.9
	$CH_{3\,ax}$	1.18s	0.36	1.2
n-Octane	CH_2 (oct)	7.23m	2.43	
	CH_3 (oct)	6.82s	2.53	0.8
	$CH_{3\,eq}$	7.14s	2.56	1.0
	$CH_{3\,ax}$	7.12s	2.49	1.1

Summary of relaxation rates for protons at different chemical shifts in nonaqueous solutions of tetramethylpiperidine-hydroxylamine.

bond dipole moment cause major changes in the effective environment as sensed by the oxygen. If the hydroxyl amine adds a hydrogen bonding position for water which would increase the steric exclusion of oxygen from this part of the molecule, then, in the present measurements we would observe an oxygen concentration that would be reduced compared with that appropriate to the nitroxide and we would underestimate the concentration differences that would be detected were the paramagnetic nitroxides observable in a high resolution NMR spectrum. If we assume that the hydroxyl amines are very similar to corresponding nitroxides with respect to the interaction with oxygen in aqueous and nonaqueous environments, then comparisons of oxygen induced nitroxide-electron relaxation rate changes may underestimate the effective oxygen concentration differences between the bulk aqueous phase and a hydrocarbon. For example, the present data suggest that if one used the oxygen induced relaxation of a nitroxide in water to compare with the oxygen induced relaxation in a phospholipid membrane interior, the difference in oxygen concentrations may be underestimated by at least a factor of 2. We note, however, that the chloroform result implies that intermolecular effects may be subtle and not easily forecasted or explained by simple arguments based on dielectric constant differences or hydrophobic effect assumptions.

Acknowledgment

This work was supported by the National Institutes of Health, EB002054.

References

[1] K. Matsumoto, B. Chandrika, J.A. Lohman, J.B. Mitchell, M.C. Krishna, S. Subramanian, Application of continuous-wave EPR spectral-spatial image reconstruction techniques for in vivo oxymetry: comparison of projection reconstruction and constant-time modalities, Magn. Reson. Med. 50 (2003) 865–874.

[2] K. Golman, J.S. Petersson, J.H. Ardenkjaer-Larsen, I. Leunbach, L.G. Wistrand, G. Ehnholm, K. Liu, Dynamic in vivo oxymetry using overhauser enhanced MR imaging, J. Magn. Reson. Imag. 12 (2000) 929–938.

[3] W.K. Subczynski, J.S. Hyde, Membranes. Barriers or pathways for oxygen transport, Adv. Exper. Med. Biol. 454 (1998) 399–408.

[4] M. Afeworki, N.R. Miller, N. Devasahayam, J. Cook, J.B. Mitchell, S. Subramanian, M.C. Krishna, Preparation and EPR studies of lithium phthalocyanine radical as an oxymetric probe, Free Radic. Biol. Med. 25 (1998) 72–78.

[5] S. Bates, Z. Yetkin, A. Jesmanowicz, J.S. Hyde, P.A. Bandettini, L. Estkowski, V.M. Haughton, Artifacts in functional magnetic resonance imaging from gaseous oxygen, J. Magn. Reson. Imag. 5 (1995) 443–445.

[6] I. Ashikawa, J.J. Yin, W.K. Subczynski, T. Kouyama, J.S. Hyde, A. Kusumi, Molecular organization and dynamics in bacteriorhodopsin-rich reconstituted membranes: discrimination of lipid environments by the oxygen transport parameter using a pulse ESR spin-labeling technique, Biochemistry 33 (1994) 4947–4952.

[7] W.K. Subczynski, L.E. Hopwood, J.S. Hyde, Is the mammalian cell plasma membrane a barrier to oxygen transport? J. Gen. Physiol. 100 (1992) 69–87.

[8] W.K. Subczynski, G.E. Renk, R.K. Crouch, J.S. Hyde, A. Kusumi, Oxygen diffusion-concentration product in rhodopsin as observed by a pulse ESR spin labeling method, Biophys. J. 63 (1992) 573–577.

[9] W.K. Subczynski, J.S. Hyde, A. Kusumi, Effect of alkyl chain unsaturation and cholesterol intercalation on oxygen transport in membranes: a pulse ESR spin labeling study, Biochemistry 30 (1991) 8578–8590.

[10] W.K. Subczynski, J.S. Hyde, A. Kusumi, Oxygen permeability of phosphatidylcholine–cholesterol membranes, Proc. Natl. Acad. Sci. USA 86 (1989) 4474–4478.

[11] B.L. Zhao, X.J. Li, R.G. He, W.Y. Jia, W.J. Xin, ESR studies on oxygen consumption during the respiratory burst of human polymorphonuclear leukocytes, Cell Biol. Int. Rep. 13 (1989) 317–323.

[12] N. Dan, X.J. Li, B.L. Zhao, T.M. Zhang, W.J. Xin, Scavenging effects of probimane on active oxygen free radicals by electron spin resonance, Zhongguo Yao Li Xue Bao/Acta Pharmacol. Sin. 10 (1989) 443–447.

[13] W.K. Subczynski, J.S. Hyde, Diffusion of oxygen in water and hydrocarbons using an electron spin resonance spin-label technique, Biophys. J. 45 (1984) 743–748.

[14] W.K. Subczynski, J.S. Hyde, Concentration of oxygen in lipid bilayers using a spin-label method, Biophys. J. 41 (1983) 283–286.

[15] W.K. Subczynski, J.S. Hyde, The diffusion-concentration product of oxygen in lipid bilayers using the spin-label T1 method, Biochim. Biophys. Acta 643 (1981) 283–291.

[16] W.L. Hubbell, D.S. Cafiso, C. Altenbach, Identifying conformational changes with site-directed spin labeling, Nat. Struct. Biol. 7 (2000) 735–739.

[17] W.L. Hubbell, H.S. McHaourab, C. Altenbach, M.A. Lietzow, Watching proteins move using site-directed spin labeling, Structure 4 (1996) 779–783.

[18] G.E. Fanucci, N. Cadieux, C.A. Piedmont, R.J. Kadner, D.S. Cafiso, Structure and dynamics of the beta-barrel of the membrane transporter BtuB by site-directed spin labeling, Biochemistry 41 (2002) 11543–11551.

[19] N.J. Malmberg, D.R. Van Buskirk, J.J. Jalke, Membrane-docking loops of the cPLA2 C2 domain: detailed structural analysis of the protein–membrane interface via site-directed spin-labeling, Biochemistry 42 (2003) 13227–13240.

[20] K.J. Oh, S. Barbuto, N. Meyer, R.-S. Kim, R.J. Collier, S.J. Korsmeyer, Conformational changes in BOD, a pro-apoptotic BCL-2 family member, upon membrane binding, J. Biol. Chem. 280 (2005) 753–767.

[21] A.J. Ozinskas, A.M. Bobst, Formation of *N*-hydroxyamines of spin labeled nucleosides for ^1H NMR analysis, Helvet. Chim. Acta 63 (1980) 1407–1411.

[22] T.L. Lee, J.F.W. Keana, In situ reduction of nitroxide spin labels with phenlhydrazine in deuteriochloroform solution. A convenient method

for obtaining structural information on nitroxides using Nuclear magnetic resonance spectroscopy. 1, J. Org. Chem. 40 (1975) 3145–3147.

[23] C.-L. Teng, S. Martini, R.G. Bryant, Local measures of intermolecular free energies in aqueous solutions, J. Am. Chem. Soc. 126 (2004) 15253–15257.

[24] C.L. Teng, R.G. Bryant, Oxygen accessibility to ribonuclease A: quantitative interpretation of nuclear spin relaxation induced by a freely diffusing paramagnet. J. Phys. Chem. (2005), in press.

[25] C.L. Teng, H. Hong, S. Kiihne, R.G. Bryant, Molecular oxygen spin–lattice relaxation in solutions measured by proton magnetic relaxation dispersion, J. Magn. Reson. 148 (2001) 31–34.